CFD Letters

Journal homepage:
https://semarakilmu.com.my/journals/index.php/CFD_Letters/index
ISSN: 2180-1363

# Poiseuille Flow of the Suspension of Gold Nanoparticles in Second-grade Fluid: Analytical Solutions

Venkat Rao Kanuri[1,2,*], K.V.Chandra Sekhar[3], P.S.Brahmanandam[4], Althada Ramesh Babu[5]

[1] Department of Mathematics, Koneru Lakshmaiah Education Foundation, Vaddeswaram –- 522302, India
[2] Department of Mathematics, SRKR Engineering College(A), Bhimavaram-534204, India
[3] Department of Mathematics, Koneru Lakshmaiah Education Foundation, Vaddeswaram- 522302, India
[4] Department of Basic Sciences, Shri Vishnu Engineering College for Women(A), Bhimavaram-534202, India
[5] Department of Humanities and Basic Sciences, Aditya University, Surampalem – 533437, India

**ARTICLE INFO**

***Article history:***
Received 16 January 2024
Received in revised form 14 February 2024
Accepted 14 March 2024
Available online 30 September 2024

***Keywords:***
Poiseuille flows; Newtonian fluids; Second-grade fluid; Volume fraction; Gold Nanoparticles; Navier-Stokes' equations

**ABSTRACT**

The Poiseuille flows have been extensively restricted to Newtonian fluids through a channel, and the significance of such flows has spanned several industries, from chemical industries to engineering applications. The restriction to Newtonian flows has impacted the further advancement in the study of Poiseuille flow and as a result, studies on Poiseuille flows have been neglected for decades. In this study, the Poiseuille flow of the second-grade nanofluid fluid is considered. The base fluid is the viscoelastic Second-grade fluid, a fluid that is both shear-thinning and shear-thickening under different conditions and whose applications can be found in polymer processing and cosmetic production. This study invokes the general assumptions of Poiseuille flow, which reduces the governing equations to ordinary differential equations. The results from simulating the model show that the velocity drops as both the second-grade fluid parameter and the volume fraction increase. The flow rate increases with increasing channel width.

## 1. Introduction

Non-Newtonian fluids exhibit a nonlinear response of shear strain to shear stress. Various examples of such fluids include the Casson fluid by Reddy and Reddy [1]; Oke *et al.,* [2], Williamson fluid by Divya *et al.,* [3], Carreau fluid by Murthy and Reddy [4], Eyring-Powell fluid by Oke *et al.,* [5], modified Eyring-Powell fluid by Oke [6, 7], and second-grade fluid by Krishna [8]. Second-grade fluids belong to the category of non-Newtonian fluids with viscoelastic properties, displaying a second-order relationship between shear stress and shear strain. They exhibit the ability to shear-thin or shear-thicken based on the specific choice of second-grade fluid. The behaviour of these fluids is influenced by both their current state and past deformation history. Examples of second-grade fluids include substances like ketchup and blood, finding applications in various industrial sectors such as pharmaceuticals, cosmetics, and polymer processing. Krishna's study [8] delved into the Hall slip on

* *Corresponding author.*
*E-mail address: k.ravi.msc@gmail.com (Venkat Rao Kanuri)*

https://doi.org/10.37934/cfdl.17.2.148162

unsteady MHD flow of second-grade fluids, revealing novel applications in aerospace science. Yavuz [9] extended partial differential equations to fractional order equations, employing Laplace transform for solving. The results indicated a reduction in velocity profile with increasing Prandtl number.

Nanofluids are engineered colloidal suspensions containing nanoparticles, typically ranging from 1 to 100 nanometres in size, dispersed within a base fluid such as water, oil, or ethylene glycol. Gold nanoparticles, due to their unique optical, thermal, and electrical properties, have garnered significant interest in nanofluid research [10]. When dispersed in a fluid, these nanoparticles can significantly alter the thermal and optical properties of the base fluid. The significance of nanofluids, particularly those containing gold nanoparticles, lies in their potential applications across various fields, including thermal management, energy harvesting, biomedical sensing, and drug delivery [11, 12]. Their enhanced thermal conductivity, optical absorption, and surface plasmon resonance properties make them promising candidates for improving heat transfer efficiency in cooling systems, enhancing the performance of photovoltaic devices, enabling sensitive detection of biomolecules, and facilitating targeted drug delivery to specific cells or tissues. This convergence of nanotechnology and fluid dynamics opens up avenues for innovative solutions in diverse areas, contributing to advancements in technology and healthcare [13-16].

Flows within a variety of pipe and channel geometries find widespread applications, typically classified as either Couette or Poiseuille flow, depending on the relative movement of the channel walls. A pressure-driven flow characterizes Poiseuille flow, while Couette flow pertains to the flow between parallel plates in relative motion by Coles [17]. In Poiseuille flow, non-overlapping layers of viscous fluid, known as laminar flow, are sustained by pressure variation by Gee & Gracie [18]. The velocity profile in Poiseuille flow takes the form of a symmetrical parabola, with a maximum point at the midpoint and no flow on the wall by Wu *et al.,* [19]. Poiseuille flow plays a crucial role in the design and development of microfluidic devices, as the velocity gradient in this profile enhances material transport. Beyond microfluidics, Poiseuille flow finds real-world applications in various industrial processes and blood flow through capillaries. It serves as a valuable tool for mimicking capillary blood flow and simulating processes like fluid transport in pipelines, heat exchanger systems, and chemical reactors, with implications for the petroleum industry and other large-scale enterprises by Sulaimon [20]. The elegance in obtaining solutions for Poiseuille flow makes it easily adaptable for sophisticated medical diagnostics, medication delivery, and microscale chemical analysis.

In this study, the Poiseuille flow of a second-grade fluid carrying gold nanoparticles is investigated. The flow is considered as it flows through a stationary channel. The novelty of this study includes the fact that it is a Poiseuille nanofluid flow, which is an extension of the classic Newtonian Poiseuille flow. The flow is modelled using the Navier-Stokes equations, and the boundary conditions are used to reduce the problem to ordinary differential equations, which are solved using appropriate methods. The following questions are answered in this study;

(i) How does volume fraction affect the flow velocity in a second-grade nanofluid flow through a channel?
(ii) How does dynamic viscosity affect the flow rate in a second-grade nanofluid flow through a channel?

## 2. Flow Description and Model Development

A pipe in two dimensions is represented as two parallel plates separated by a certain distance. Consider a 2D channel, as shown in Figure 1, separated by a distance of $2h$ such that the flow is symmetrical about the axis of flow $y = 0$. A second-grade fluid in which a nanoparticle is suspended undergoes a steady incompressible flow through the channel. This study considers a fully developed flow of such a system.

### *2.1 The Governing Equations*

By following the Navier-Stokes' equations, the following governing equations include the continuity equation and the momentum equation. Adopting the studies of Sitamahalakshmi *et al.,* [21], Kọríkọ *et al.,* [22] and Oke *et al.,* [2], we have the governing equations as

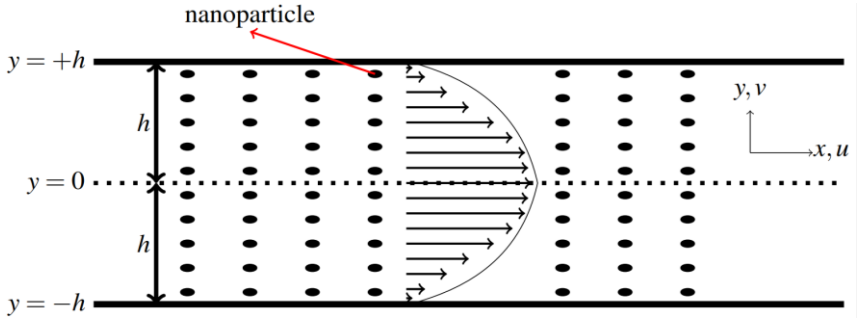


**Fig. 1.** Flow configuration

$$\nabla \cdot \vec{\boldsymbol{V}} = 0, \tag{1}$$

$$\rho_{nf}\left(\frac{\partial \vec{\boldsymbol{V}}}{\partial t} + \left(\vec{\boldsymbol{V}} \cdot \nabla\right)\vec{\boldsymbol{V}}\right) = \nabla \cdot \boldsymbol{\sigma} + \rho_{nf} b, \tag{2}$$

Where $\vec{\boldsymbol{V}} = (u_1, u_2, u_3)$ is the velocity vector, $\nabla$ is the gradient operator in 3-dimensions defined as

$$\vec{\nabla} = i\frac{\partial}{\partial x_1} + j\frac{\partial}{\partial x_2} + k\frac{\partial}{\partial x_3},$$

$\boldsymbol{\sigma}$ is the stress tensor, $b$ is body forces. Steady flow is independent of time and Eq. (2) becomes

$$\left(\vec{\boldsymbol{V}} \cdot \nabla\right)\vec{\boldsymbol{V}} = \frac{1}{\rho_{nf}}\nabla \cdot \boldsymbol{\sigma} + b \tag{3}$$

The second-grade nanofluid stress tensor follows the form

$$\boldsymbol{\sigma} = -p\boldsymbol{I} + \mu_{nf}\boldsymbol{A}_1 + \alpha_1\boldsymbol{A}_2 + \alpha_2\boldsymbol{A}_1^2, \tag{4}$$

(See [23-25]), where $\boldsymbol{I}$ is the identity tensor $p$ is the pressure, $\mu_{nf}$ is the dynamic viscosity of the nanofluid. $\boldsymbol{A}_1, \boldsymbol{A}_2$ are the Rivillin Ericksen tensors defined for steady flow as

$$\boldsymbol{A}_1 = \nabla \boldsymbol{V} + (\nabla \boldsymbol{V})^T, \qquad \boldsymbol{A}_2 = (\boldsymbol{V} \cdot \nabla)\boldsymbol{A}_1 + \boldsymbol{A}_1(\nabla \boldsymbol{V}) + \left(\boldsymbol{A}_1^T(\nabla \boldsymbol{V})\right)^T \tag{5}$$

Using the tensor notation, we have

$$\nabla \boldsymbol{V} = \left(\partial_i u_j\right), \quad i,j = 1,2,3$$

and consequently,

$$\boldsymbol{A}_1 = \left(\partial_i u_j + \partial_j u_i\right), \quad i,j = 1,2,3.$$

The flow under consideration is happening only in the $y$-direction and as a result velocity components in the $x$ and $z$ directions are both zeros, which indicates that $u_2 = u_3 = 0$. Eq. (1) is therefore reduced to

$$\frac{\partial u_1}{\partial x_1} = 0, \tag{6}$$

And

$$\boldsymbol{\sigma} = \begin{pmatrix} -p & \mu_{nf}\partial_2 u_1 & 0 \\ \mu_{nf}\partial_2 u_1 & -p + (2\alpha_1 + \alpha_2)(\partial_2 u_1)^2 & 0 \\ 0 & 0 & -p \end{pmatrix} \tag{7}$$

Hence,

$$\nabla \cdot \boldsymbol{\sigma} = \left(-\partial_1 p + \partial_2\left(\mu_{nf}\partial_2 u_1\right), \ -\partial_2 p + 2(2\alpha_1 + \alpha_2)\partial_2 u_1 \partial_2^2 u_1, \ -\partial_3 p\right) \tag{8}$$

Setting the second-grade parameter as $\lambda = 2(2\alpha_1 + \alpha_2)$ and replacing the directions as

$$x_1 = x, \qquad x_2 = y, x_3 = z,$$

Observing Eq. (6), then we can rewrite the momentum equations as

$$0 = -\frac{1}{\rho_{nf}}\frac{\partial p}{\partial x} + \frac{\mu_{nf}}{\rho_{nf}}\frac{\partial^2 u}{\partial y^2}, \tag{9}$$

$$0 = -\frac{1}{\rho_{nf}}\frac{\partial p}{\partial y} + \lambda\frac{\partial u}{\partial y}\frac{\partial^2 u}{\partial y^2}, \tag{10}$$

$$0 = -\frac{1}{\rho_{nf}}\frac{\partial p}{\partial z}. \tag{11}$$

*2.2 Initial and Boundary Conditions*

The boundary conditions for the flow will include the no-slip conditions at the wall. This condition ensures that the fluid layers glued to the wall maintain the same velocity as the channel and that the

fluid particles do not slide away. In this flow, the channel is not moving, and as a result, the wall velocity is zeros. This condition is observed at the two ends of the pipe (that is, at $y = +h$ and $y = -h$) and we, therefore have the no-slip boundary condition represented as

$$u(+h) = 0 \quad \text{and} \quad u(-h) = 0$$

From practical observation, the fluid flow attains the maximum velocity on the axis of the symmetrical flow (that is, at $y = 0$). From calculus, the maximum velocity is obtained at a point where the derivative is zero. To represent this condition, we write it as

$$\left.\frac{\partial u}{\partial y}\right|_{y=0} = 0$$

*2.3 Thermophysical Properties*

As a nanofluid, both the base fluid and the nanoparticles contribute to the electrical and thermal properties of the flow. Hence, it is important to consider the effective properties of the flow. According to Oke *et al.,* [6], the volume fraction has a significant influence on the dynamic viscosity and the density of the resulting nanofluid. The ratio of the nanofluid dynamic viscosity to base fluid dynamic viscosity is estimated to be

$$\begin{aligned} &\frac{\mu_{nf}}{\mu_{bf}} = 0.904\exp(0.148\phi), \\ &\Rightarrow \quad \mu_{nf} = 0.904\mu_{bf}\exp(0.148\phi), \end{aligned} \tag{12}$$

Where the nanoparticle volume fraction is represented as $\phi$ and the dynamic viscosity for the base fluid is $\mu_{bf}$. The ratio of the nanofluid density to the base fluid density is given, according to Oke [26, 27], as

$$\begin{aligned} &\frac{\rho_{nf}}{\rho_{bf}} = 1 - \phi + \phi\frac{\rho_{np}}{\rho_{bf}}, \\ &\Rightarrow \ \rho_{nf} = \left(1 - \phi + \phi\frac{\rho_{np}}{\rho_{bf}}\right)\rho_{bf} \end{aligned} \tag{13}$$

For simplicity, we set

$$\eta = 0.904\exp(0.148\phi)\,, \ \ \xi = \left(1 - \phi + \phi\frac{\rho_{np}}{\rho_{bf}}\right), \tag{14}$$

and so,

$$\mu_{nf} = \eta\mu_{bf}, \quad \rho_{nf} = \xi\rho_{bf} \quad \text{and} \quad \frac{\mu_{nf}}{\rho_{nf}} = \frac{\eta\mu_{bf}}{\xi\rho_{bf}} \tag{15}$$

The second-grade fluid chosen for this study is blood and the nanoparticle chosen is the gold nanoparticle. The physical properties as found in Azmi *et al.,* [28] are provided in Table 1.

**Table 1**
Thermophysical properties

| | Blood | Gold |
|---|---|---|
| Density $[ML^{-3}]$ | 1063 | 19300 |
| Viscosity $[ML^{-1}T^{-1}]$ | 3.5-5.5 | – |

Making the substitutions Eq. (14) and Eq. (15), the governing equation is therefore rewritten as

$$0 = -\frac{1}{\xi\rho_{bf}}\frac{\partial p}{\partial x} + \frac{\eta\mu_{bf}}{\xi\rho_{bf}}\frac{\partial^2 u}{\partial y^2}, \tag{16}$$

$$0 = -\frac{1}{\xi\rho_{bf}}\frac{\partial p}{\partial y} + \lambda\frac{\partial u}{\partial y}\frac{\partial^2 u}{\partial y^2}, \tag{17}$$

$$0 = -\frac{1}{\xi\rho_{bf}}\frac{\partial p}{\partial z}, \tag{18}$$

With the conditions

$$u(+h) = 0, \;\; u(-h) = 0, \;\; \text{and} \;\; \left.\frac{\partial u}{\partial y}\right|_{y=0} = 0 \tag{19}$$

## 3. Exact Solution

The indication of Eq. (18) where the rate of change of pressure with length is zero is that pressure is constant in the $z$-direction. Now,

$$0 = -\frac{1}{\xi\rho_{bf}}\frac{\partial p}{\partial z} \quad \Rightarrow 0 = \frac{\partial p}{\partial z}$$
$$\Rightarrow p = p(x, y) \tag{20}$$

Also, from Eq. (16)

$$0 = -\frac{1}{\xi\rho_{bf}}\frac{\partial p}{\partial x} + \frac{\eta\mu_{bf}}{\xi\rho_{bf}}\frac{\partial^2 u}{\partial y^2},$$
$$\Rightarrow \quad \frac{\eta\mu_{bf}}{\xi\rho_{bf}}\frac{\partial^2 u}{\partial y^2} = \frac{1}{\xi\rho_{bf}}\frac{\partial p}{\partial x},$$
$$\Rightarrow \quad \frac{\partial^2 u}{\partial y^2} = \frac{1}{\eta\mu_{bf}}\frac{\partial p}{\partial x}. \tag{21}$$

Putting Eq. (21) in Eq. (17) gives

$$0 = -\frac{1}{\xi\rho_{bf}}\frac{\partial p}{\partial y} + \lambda\frac{\partial u}{\partial y}\left(\frac{1}{\eta\mu_{bf}}\frac{\partial p}{\partial x}\right),$$
$$\Rightarrow \quad \frac{\lambda}{\eta\mu_{bf}}\frac{\partial p}{\partial x}\frac{\partial u}{\partial y} = \frac{1}{\xi\rho_{bf}}\frac{\partial p}{\partial y},$$

$$\Rightarrow \quad \frac{\partial u}{\partial y} = \frac{\eta \mu_{bf}}{\lambda \xi \rho_{bf}} \left( \frac{\partial p}{\partial y} \div \frac{\partial p}{\partial x} \right), \tag{22}$$

From Eq. (20), $p = p(x, y)$, hence considering a pressure distribution of the form

$$p(x, y) = x^2 + y^2 = h^2.$$

Then

$$\frac{\partial p}{\partial y} \div \frac{\partial p}{\partial x} = \frac{2y}{2x} = \frac{y}{x},$$

and consequently,

$$\frac{\partial u}{\partial y} = -\frac{\eta \mu_{bf}}{\lambda \xi \rho_{bf}} \frac{y}{x}.$$

On integrating both sides

$$\int_{s=-h}^{s=y} \frac{\partial u}{\partial s} ds = -\int_{s=-h}^{s=y} \frac{\eta \mu_{bf}}{\lambda \xi \rho_{bf}} \frac{s}{x} ds,$$

(replacing $y$ with $s$ in the integral to avoid conflict with the limit), we have

$$\begin{aligned} u(s)|_{s=-h}^{s=y} &= -\frac{\eta \mu_{bf}}{\lambda \xi \rho_{bf}} \left( \frac{s^2}{2x} \Big|_{s=-h}^{s=y} \right), \\ u(y) - u(-h) &= -\frac{\eta \mu_{bf}}{\lambda \xi \rho_{bf}} \left( \frac{y^2}{2x} - \frac{h^2}{2x} \right), \\ u(y) &= -\frac{\eta \mu_{bf}}{2x \lambda \xi \rho_{bf}} (y^2 - h^2). \end{aligned} \tag{23}$$

The other two conditions are automatically satisfied since

$$\begin{aligned} u(+h) &= -\frac{\eta \mu_{bf}}{2x \lambda \xi \rho_{bf}} (h^2 - h^2) = 0, \\ \frac{du}{dy} &= -\frac{\eta \mu_{bf} y}{x \lambda \xi \rho_{bf}} \quad \Rightarrow \frac{du}{dy}\Big|_{y=0} = 0. \end{aligned}$$

From the pressure distribution, it is clear that

$$x = \sqrt{y^2 - h^2},$$

and so, the velocity is

$$u(y) = -\frac{\eta\mu_{bf}}{2\lambda\xi\rho_{bf}\sqrt{y^2-h^2}}(y^2-h^2),$$
$$u(y) = \frac{\eta\mu_{bf}}{2\lambda\xi\rho_{bf}\sqrt{y^2-h^2}}(h^2-y^2),$$
$$u(y) = \frac{\eta\mu_{bf}}{2\lambda\xi\rho_{bf}}\sqrt{h^2-y^2}.$$

The rate of flow of nanofluid within a pipe of diameter $2h$ is

$$\begin{aligned}
q &= \int_{-h}^{h} u dy, \\
&= \frac{\eta\mu_{bf}}{2\lambda\xi\rho_{bf}}\int_{-h}^{h}\sqrt{h^2-y^2}dy, \\
&= \frac{\eta\mu_{bf}}{2\lambda\xi\rho_{bf}}\int_{-\frac{\pi}{4}}^{\frac{\pi}{4}} h^2\cos^2\theta\, d\theta, \quad (\text{using the substitution } y = h\sin\theta) \\
&= \frac{\eta\mu_{bf}h^2}{2\lambda\xi\rho_{bf}}\frac{1}{2}\left(\theta + \frac{\sin(2\theta)}{2}\right)_{-\frac{\pi}{4}}^{\frac{\pi}{4}}, \\
&= \frac{\eta\mu_{bf}h^2}{4\lambda\xi\rho_{bf}}\left(\left(\frac{\pi}{4} + \frac{\sin\left(\frac{\pi}{2}\right)}{2}\right) - \left(-\frac{\pi}{4} + \frac{\sin\left(-\frac{\pi}{2}\right)}{2}\right)\right), \\
&= \left(1+\frac{\pi}{2}\right)\frac{\eta\mu_{bf}h^2}{4\lambda\xi\rho_{bf}}.
\end{aligned}$$

Compiling the results, we have the flow velocity as

$$u(y) = \frac{\eta\mu_{bf}}{2\lambda\xi\rho_{bf}}\sqrt{h^2-y^2}, \tag{24}$$

and the rate of flow as

$$q = \left(1+\frac{\pi}{2}\right)\frac{\eta\mu_{bf}h^2}{4\lambda\xi\rho_{bf}} \tag{25}$$

Where

$$\eta = 0.904\exp(0.148\phi), \quad \xi = \left(1-\phi+\phi\frac{\rho_{np}}{\rho_{bf}}\right) \tag{26}$$

And $q[L^2T^{-1}]$ is the rate of flow, $\phi$ is the dimensionless volume fraction, $h$ $[L]$ is the channel radius $\lambda$ $[L^2]$ is the second-grade fluid parameter, $\rho_{np}$ and $\rho_{bf}$ $[ML^{-3}]$ the density of the nanoparticle and the base-fluid respectively.

## 4. Analysis and Discussion of Results

Numerical simulation refers to experimenting with different values of the parameters to see how they influence the behaviour of the variables. The MATLAB software was adopted for the numerical solution and the graphical illustrations of the results. In this case, the parameters of interest are the fluid parameter $\lambda$, volume fraction $\phi$ and the channel radius $h$. As a necessary condition, we establish the parabolic nature of the velocity to ascertain the Poiseuille nature of the flow. Figure 2 show that the velocity and flow rate are parabolic, with the highest velocity attained at the centre and the flow rate increasing with increasing channel radius.

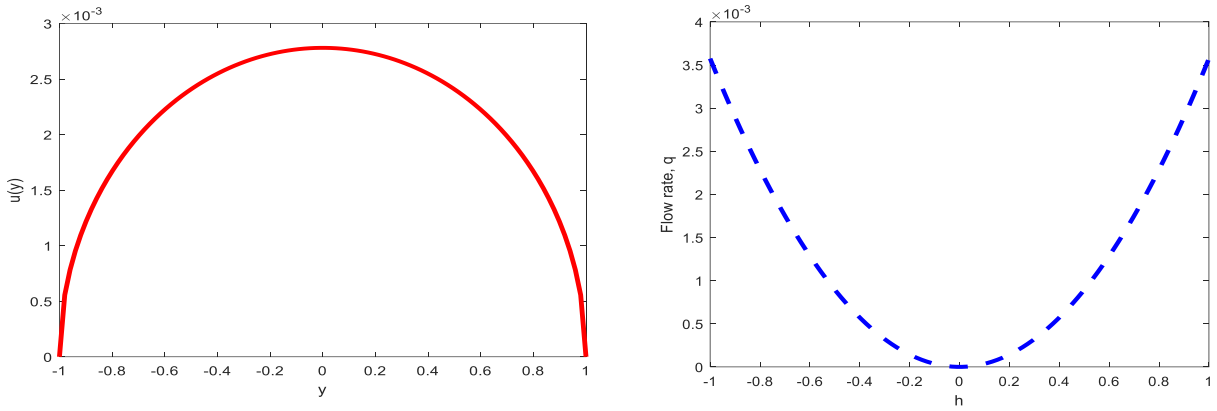


(a) (b)

**Fig. 2.** Figure (a) Velocity (b) flow rate profiles with $h = 1, \mu_{bf} = 3.5, \lambda = 0.2, \phi = 0.1$

The simulation is carried out with default values of the parameters set as

$$h = 1, \ \mu = 3.5, \ \lambda = 0.2$$

One parameter is varied, while others are fixed and the results are discussed below.

### *4.1 Variation of Velocity with the Parameters*

This section exhibits the velocity distribution of the gold-blood nanofluid flow through a stationary channel as the parameters are varied. Figure 3 shows that the velocity drops gradually as the fluid parameter increases. Increasing $\lambda$ implies that the flow becomes more viscous and, more fluid layers are dragged by the viscous force. The more layers of fluid are affected by the drag, the slower the fluid flows. This explains the observation in Figure 3. The effect of volume fraction on velocity distribution is shown in Figure 4. It is observed that velocity drops as volume fraction increases. Volume fraction represents the percentage of the fluid volume that is made up of the nanoparticles. Any increment in the volume fraction simply means more nanoparticles are present in the fluid. Gold nanoparticles are heavier than fluid particles and tend to settle down in the channel. The agglomeration of the gold nanoparticles can result in clogging and blockage of the pipe, which consequently leads to a reduced flow velocity as shown in Figure 4. Hence, increasing the volume fraction will lead to a reduction in the flow velocity. The viscosity of blood varies from 3.5 to $5.5 kg\, m^{-1}\, s^{-1}$. By varying the values of $\mu_{bf}$ in the interval $[3.5, 5.5]$, the velocity distribution is plotted in Figure 5 indicating an increasing velocity with increasing dynamic viscosity of the base-fluid.

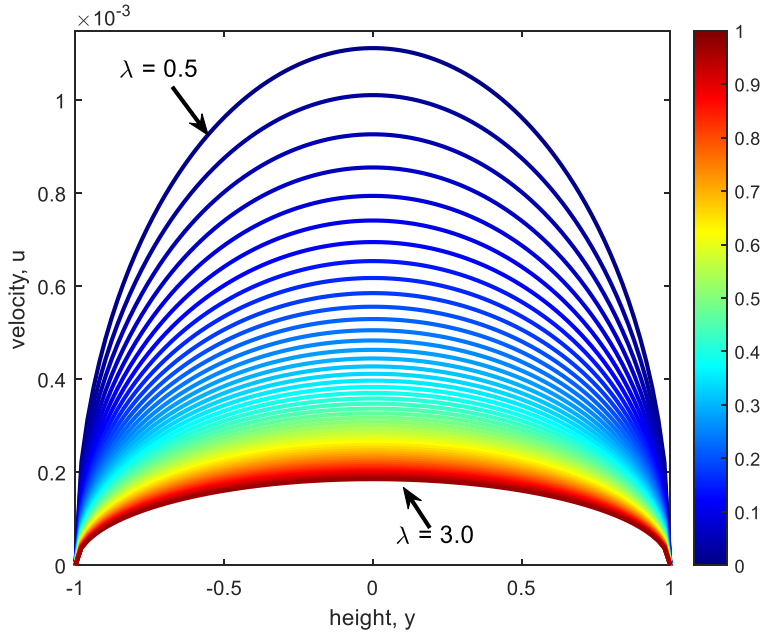


**Fig. 3.** Velocity distribution for various λ

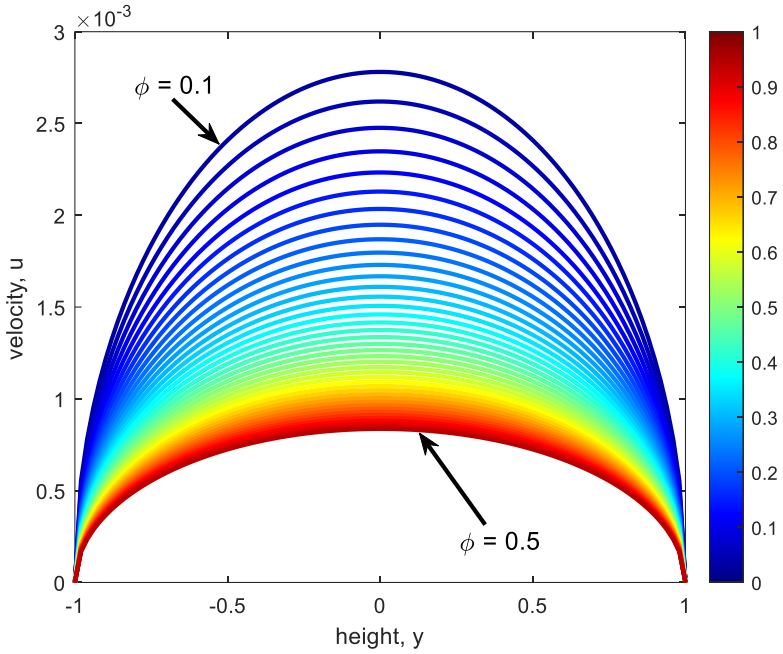


**Fig. 4.** Velocity distribution for ϕ

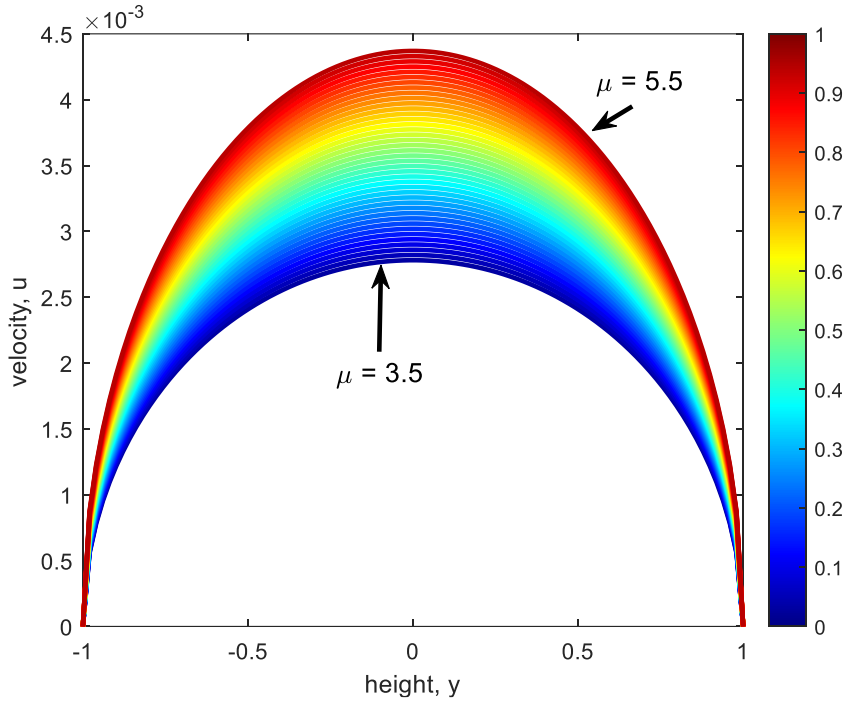


**Fig. 5.** Velocity distribution for $\mu_{bf}$

### *4.2 Variation of Flow Rate with the Parameters*

This section exhibits the flow rate of the gold-blood nanofluid through a $2h$-diameter stationary channel as the parameters are varied. Each parameter is varied several times at a fixed $h$ and the flow rate is recorded each time so that the flow rate is plotted against the varying parameters. The process is repeated for several fixed values of $h$ and the resulting graphs are shown in Figures 6 – 8. The flow rate represents the volume of nanofluid that goes through a cross-sectional area of the channel at a time. Figure 6 shows that the flow rate reduces with increasing fluid parameters whereas the flow rate increases with increasing channel radius. As the channel radius increases, more fluid can move through the channel at any given time, and that explains the reason for the rise in the flow rate as the flow radius increases (see Figure 6). The flow rate goes down as the fluid becomes more viscous (that is, as $\lambda$ increases) due to the increase in the number of fluid layers affected by the viscous drag. This is also depicted in Figure 6, where the flow rate decreases with $\lambda$ but increases with channel radius. Figure 7 shows that the flow rate reduces with increasing volume fraction. The agglomeration of nanoparticles in the channel caused due to the increasing volume fraction will reduce the amount of fluid that can flow through a certain cross-sectional area and hence, a decreasing flow rate. Figure 8 shows that as viscosity increases, the flow rate increases.

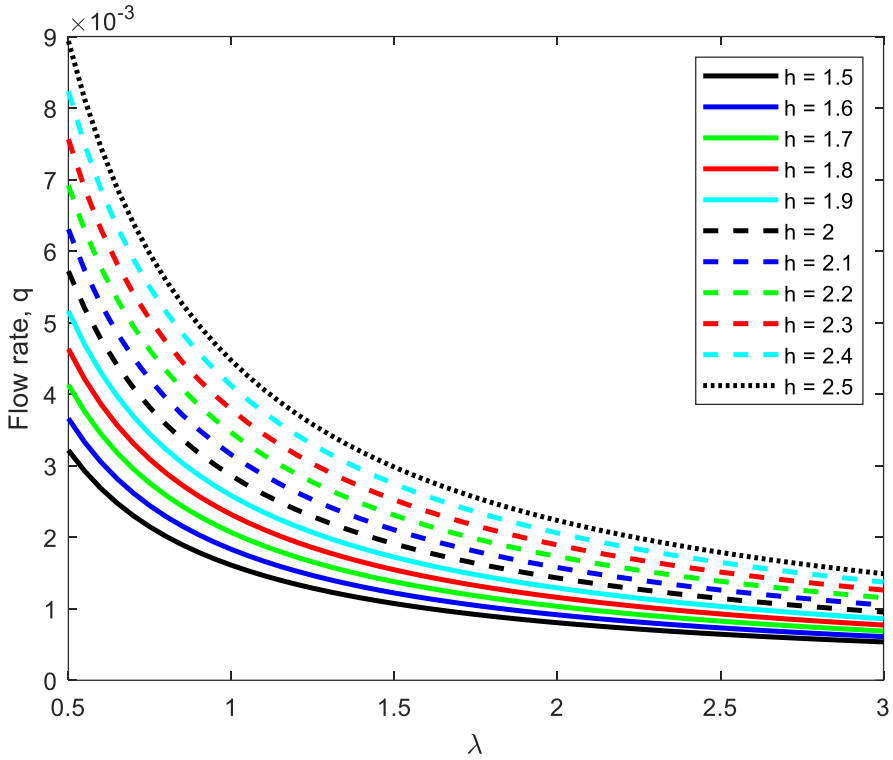


**Fig. 6.** Flow rate with λ at different h

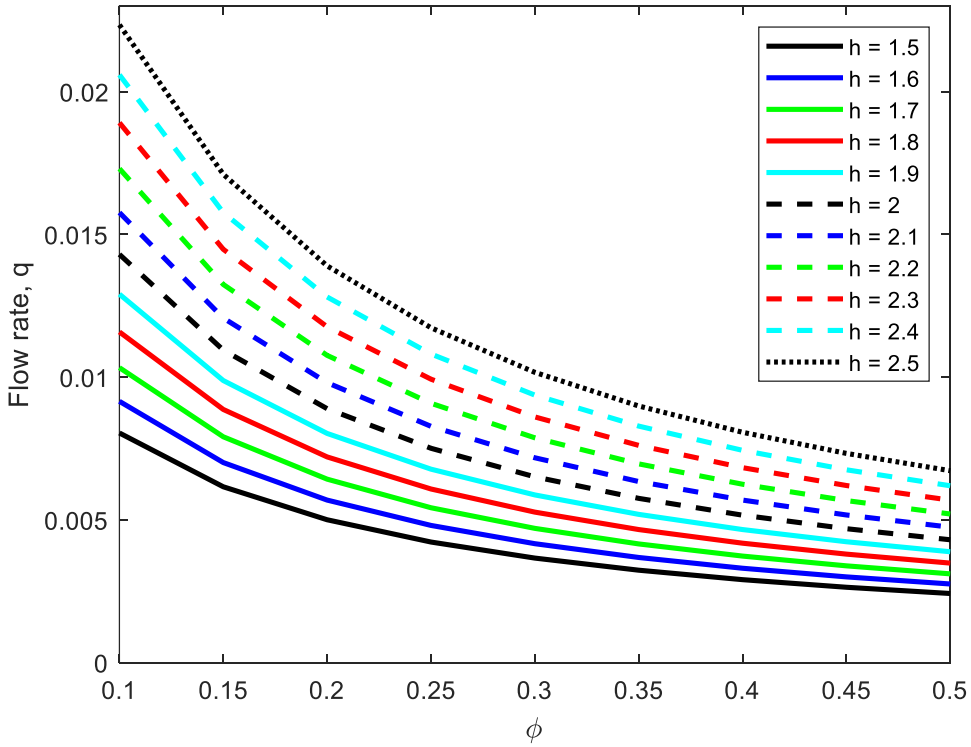


**Fig. 7.** Flow rate with ϕ at different $h$

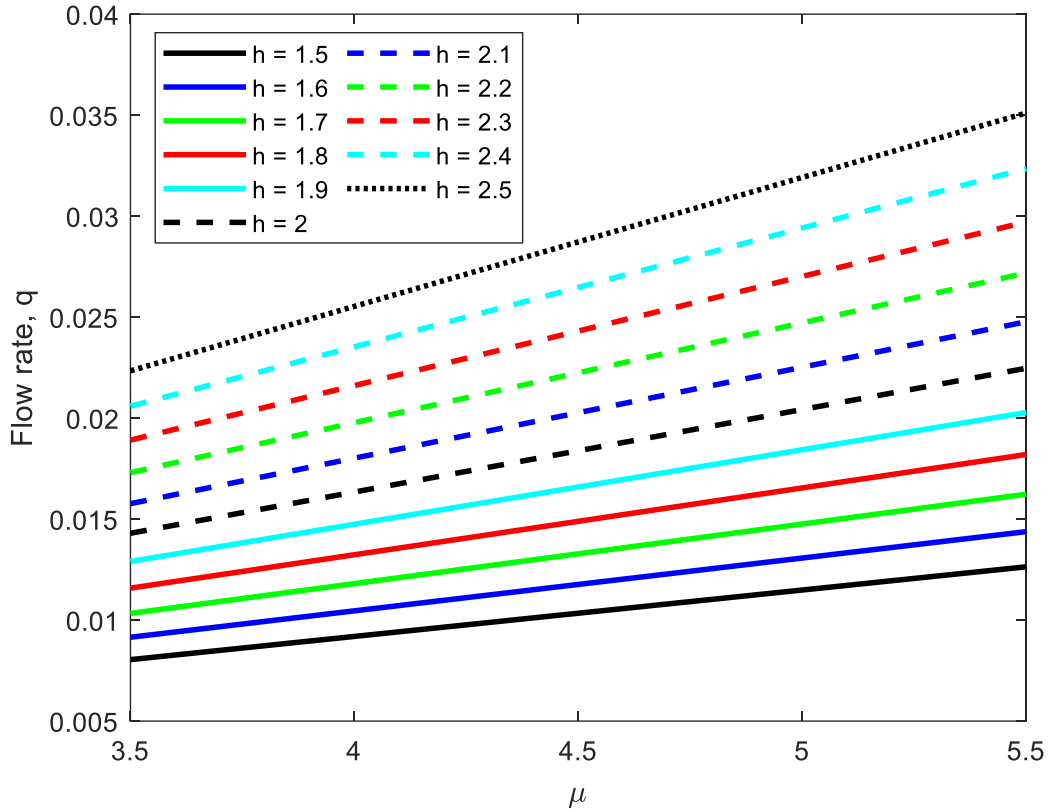


**Fig. 8.** Flow rate with μ at different $h$

## 5. Conclusion

The flow of a suspension of gold nanoparticles in the blood is considered within a channel of diameter $2h$. The governing equations are derived alongside the boundary and initial conditions. The analytical solution is sought by adopting the methods of solving ordinary differential equations. Simulation of the model shows the following;

i. There is a velocity drop as the second-grade fluid parameter and volume fraction increase.
ii. The velocity rises as the dynamic viscosity of the base fluid increases.
iii. Flow rate reduces with increasing fluid parameters.
iv. The flow rate increases with increasing channel radius.
v. The flow rate goes down as the fluid becomes more viscous.
vi. The flow rate reduces with increasing volume fraction.

## Acknowledgement

"This research was not funded by any grant"

## References

[1] Reddy, Karnati Veera, and Gurrampati Venkata Ramana Reddy. "Outlining the impact of melting on mhd casson fluid flow past a stretching sheet in a porous medium with radiation." *Biointerface Research in Applied Chemistry* 13 (2022): 1-14. https://doi.org/10.33263/BRIAC131.042

[2] Oke, Abayomi S., Winifred N. Mutuku, Mark Kimathi, and Isaac L. Animasaun. "Insight into the dynamics of non-Newtonian Casson fluid over a rotating non-uniform surface subject to Coriolis force." *Nonlinear Engineering* 9, no. 1 (2020): 398-411. https://doi.org/10.1515/nleng-2020-0025

[3] Divya, G. Poorna, G. V. Reddy, and P. Bindu. "Unsteady MHD Casson and Williamson nanofluids over a permeable stretching sheet in the presence of thermal radiation and chemical reaction." In *AIP Conference Proceedings*, vol. 2707, no. 1. AIP Publishing, 2023. https://doi.org/10.1063/5.0143359

[4] Murthy, C. V., and G. Reddy. "MHD Casson And Carreau Fluid Flow Through A Porous Medium With Variable Thermal Conductivity In The Presence Of Suction/Injection." *Journal of Naval Architecture & Marine Engineering* 20, no. 1 (2023).

[5] Oke, Abayomi S., Temitope Eyinla, and Belindar A. Juma. "Effect of Coriolis force on modified Eyring Powell fluid flow." *Journal of Engineering Research and Reports* 24, no. 4 (2023): 26-34.https://doi.org/10.9734/jerr/2023/v24i4811

[6] Oke, A. S., I. L. Animasaun, W. N. Mutuku, M. Kimathi, Nehad Ali Shah, and S. Saleem. "Significance of Coriolis force, volume fraction, and heat source/sink on the dynamics of water conveying 47 nm alumina nanoparticles over a uniform surface." *Chinese Journal of Physics* 71 (2021): 716-727.https://doi.org/10.1016/j.cjph.2021.02.005

[7] Oke, A. S. "Theoretical analysis of modified eyring powell fluid flow." *Journal of the Taiwan Institute of Chemical Engineers* 132 (2022): 104152.https://doi.org/10.1016/j.jtice.2021.11.019

[8] Krishna, M. Veera, N. Ameer Ahamad, and Ali J. Chamkha. "Hall and ion slip impacts on unsteady MHD convective rotating flow of heat generating/absorbing second grade fluid." *Alexandria Engineering Journal* 60, no. 1 (2021): 845-858. https://doi.org/10.1016/j.aej.2020.10.013

[9] Yavuz, Mehmet, Ndolane Sene, and Mustafa Yıldız. "Analysis of the influences of parameters in the fractional second-grade fluid dynamics." *Mathematics* 10, no. 7 (2022): 1125. https://doi.org/10.3390/math10071125

[10] Zuberi, Haris Alam, Madan Lal, Shivangi Verma, and Nurul Amira Zainal. "Computational Investigation of Brownian Motion and Thermophoresis Effect on Blood-based Casson Nanofluid on a Non-linearly Stretching Sheet." *Journal of Advanced Research in Numerical Heat Transfer* 18, no. 1 (2024): 49-67. https://doi.org/10.37934/arnht.18.1.4967

[11] Mekheimer, Kh S., A. Z. Zaher, and W. M. Hasona. "Entropy of AC electro-kinetics for blood mediated gold or copper nanoparticles as a drug agent for thermotherapy of oncology." *Chinese Journal of Physics* 65 (2020): 123-138.

[12] Ramadan, Shaimaa F., Kh S. Mekheimer, Muhammad Mubashir Bhatti, and A. M. A. Moawad. "Phan-Thien-Tanner nanofluid flow with gold nanoparticles through a stenotic electrokinetic aorta: a study on the cancer treatment." *Heat Transfer Research* 52, no. 16 (2021).

[13] Ishak, Siti Shuhada, Mohd Rijal Ilias, Seripah Awang Kechil, and Fazillah Bosli. "Aligned Magnetohydrodynamics and Thermal Radiation Effects on Ternary Hybrid Nanofluids Over Vertical Plate with Nanoparticles Shape Containing Gyrotactic Microorganisms." *Journal of Advanced Research in Numerical Heat Transfer* 18, no. 1 (2024): 68-91.https://doi.org/10.37934/arnht.18.1.6891.

[14] Oke, Abayomi S., Winifred N. Mutuku, Mark Kimathi, and Isaac Lare Animasaun. "Coriolis effects on MHD newtonian flow over a rotating non-uniform surface." *Proceedings of the Institution of Mechanical Engineers, Part C: Journal of Mechanical Engineering Science* 235, no. 19 (2021): 3875-3887.

[15] Oke, Abayomi S., and Winifred N. Mutuku. "Significance of viscous dissipation on MHD Eyring–Powell flow past a convectively heated stretching sheet." *Pramana* 95, no. 4 (2021): 199.

[16] Ouru, J. O., W. N. Mutuku, and A. S. Oke. "Buoyancy-induced MHD stagnation point flow of Williamson fluid with thermal radiation." *Journal of Engineering Research and Reports* 11, no. 4 (2020): 9-18.

[17] Coles, Donald. "Transition in circular Couette flow." *Journal of Fluid Mechanics* 21, no. 3 (1965): 385-425. https://doi.org/10.1017/S0022112065000241

[18] Gee, Bruce, and Robert Gracie. "Beyond Poiseuille flow: A transient energy-conserving model for flow through fractures of varying aperture." *Advances in Water Resources* 164 (2022): 104192. https://doi.org/10.1016/j.advwatres.2022.104192

[19] Wu, Shiwen, Zhihao Xu, Ruda Jian, Siyu Tian, Long Zhou, Tengfei Luo, and Guoping Xiong. "Molecular alignment-mediated stick–slip Poiseuille flow of oil in graphene nanochannels." *The Journal of Physical Chemistry B* 127, no. 27 (2023): 6184-6190. https://doi.org/10.1021/acs.jpcb.3c01805

[20] Sulaimon, Aliyu Adebayo, Muhammad Zaid Sannang, Masooma Nazar, and Azmi Mohd Shariff. "Investigating the effect of okra mucilage on waxy oil flow in pipeline." *Journal of Advanced Research in Fluid Mechanics and Thermal Sciences* 107, no. 2 (2023): 41-49. https://doi.org/10.37934/arfmts.107.2.4149

[21] Sitamahalakshmi, V., G. Venkata Ramana Reddy, and Bidemi Olumide Falodun. "Heat and mass transfer effects on MHD Casson fluid flow of blood in stretching permeable vessel." *J. Appl. Nonlinear Dyn* 12 (2023): 87-97. https://doi.org/10.5890/JAND.2023.03.006

[22] Kọríkọ, O. K., K. S. Adegbie, A. S. Oke, and I. L. Animasaun. "Exploration of Coriolis force on motion of air over the upper horizontal surface of a paraboloid of revolution." *Physica Scripta* 95, no. 3 (2020): 035210. https://doi.org/10.1088/1402-4896/ab4c50

[23] Ayub, M. & Zaman, H. (2010). "Complete derivation of the momentum equation for the second-grade fluid." *Journal of Mathematics and Computer Science, 1*(1), 33-39. https://doi.org/10.22436/jmcs.001.01.05

[24 Andersson, H. I. "MHD flow of a viscoelastic fluid past a stretching surface." *Acta Mechanica* 95, no. 1 (1992): 227-230. https://doi.org/10.1007/BF01170814

[25] Beard, D. W. "Two-dimensional flow near a stagnation point." In *Proc. Camb. Phil. Soc.*, vol. 60, pp. 667-674. 1964. https://doi.org/10.1017/S0305004100038147

[26] Oke, Abayomi Samuel. "Heat and mass transfer in 3D MHD flow of EG-based ternary hybrid nanofluid over a rotating surface." *Arabian Journal for Science and Engineering* 47, no. 12 (2022): 16015-16031. https://doi.org/10.1007/s13369-022-06838-x

[27] Oke, A. S. "Coriolis effects on MHD flow of MEP fluid over a non-uniform surface in the presence of thermal radiation." *International Communications in Heat and Mass Transfer* 129 (2021): 105695. https://doi.org/10.1016/j.icheatmasstransfer.2021.105695

[28] Azmi, Wan Faezah Wan, Ahmad Qushairi Mohamad, Lim Yeou Jiann, and Sharidan Shafie. "Unsteady natural convection flow of blood Casson nanofluid (Au) in a cylinder: nano-cryosurgery applications." *Scientific reports* 13, no. 1 (2023): 5799. https://doi.org/10.1038/s41598-023-30129-6